Plant Physiol. (1994) 105: 799–813

Ion Channels in the Xylem Parenchyma of Barley Roots[1]

A Procedure to Isolate Protoplasts from This Tissue and a Patch-Clamp Exploration of Salt Passageways into Xylem Vessels

Lars H. Wegner[2] and Klaus Raschke*

Pflanzenphysiologisches Institut und Botanischer Garten der Universität Göttingen, Untere Karspüle 2, 37073 Göttingen, Germany

To identify mechanisms for the simultaneous release of anions and cations into the xylem sap in roots, we investigated voltage-dependent ion conductances in the plasmalemma of xylem parenchyma cells. We applied the patch-clamp technique to protoplasts isolated from the xylem parenchyma by differential enzymic digestion of steles of barley roots (*Hordeum vulgare* L. cv Apex). In the whole-cell configuration, three types of cation-selective rectifiers could be identified: (a) one activated at membrane potentials above about −50 mV; (b) a second type of outward current appeared at membrane potentials above +20 to +40 mV; (c) below a membrane potential of approximately −110 mV, an inward rectifier could be distinguished. In addition, an anion-specific conductance manifested itself in single-channel activity in a voltage range extending from about −100 to +30 mV, with remarkably slow gating. In excised patches, K^+ channels activated at hyperpolarization as well as at depolarization. We suggest that salt is released from the xylem parenchyma into the xylem apoplast by simultaneous flow of cations and anions through channels, following electrochemical gradients set up by the ion uptake processes in the cortex and, possibly, the release and reabsorption of ions on their way to the xylem.

In roots, a vectorial transport of mineral nutrients is established: Ions are taken up from the soil solution by cortical cells (Clarkson, 1989) and move radially across the root into the xylem sap. This radial transport must be symplastic, at least in part, to circumvent the Casparian band that prevents ions from entering the stele by apoplastic diffusion. Because the conducting xylem vessels form part of the apoplast in the stele, ions have to pass the plasmalemma of xylem parenchyma cells, bordering the xylem vessels, to be released into the xylem sap. Several theories deal with the transport mechanisms involved here, but experimental evidence for each one of these theories is scarce (reviews by Pitman, 1977; Clarkson, 1989). In a pioneering paper, Crafts and Broyer (1938) proposed a passive mechanism of ion transport to the xylem, assuming that the plasmalemma was leaky due to oxygen deficiency. According to Hylmø (1953), maturing xylem vessels are the site of ion release to the xylem sap, and xylem loading is caused by the successive death of these cells. However, evidence that transport into the xylem can be inhibited selectively (Pitman, 1977, 1982) gave rise to speculations that an active transport may be involved. Hanson (1978) proposed a chemiosmotic scheme for xylem loading; according to his view, ion transport is energized by the activity of proton pumps located in the plasmalemma of xylem parenchyma cells ("stelar pump"). Using a perfusion technique, several authors (De Boer and Prins, 1985; Clarkson and Hanson, 1986; De Boer, 1989) obtained evidence for pump activity in the stele. However, coupling between proton fluxes and the transport of K^+ and anions into the xylem sap has not yet been demonstrated.

We approached the problem of salt transport into the xylem in a new way by isolating protoplasts from the xylem parenchyma and recording activities of ion currents and ion channels in their plasmalemmata, applying the patch-clamp technique of E. Neher and B. Sakmann (Hamill et al., 1981). Ion channels have been shown to be the main pathways for the uptake and release of K^+ and relevant anions during stomatal opening and closing (Schroeder et al., 1987; Keller et al., 1989; Hedrich et al., 1990; Linder and Raschke, 1992) and for K^+ efflux from motor cells in pulvini of *Samanea* (Moran et al., 1988) and *Mimosa* (Stoeckel and Takeda, 1993).

We developed a method for the selective preparation of protoplasts from the xylem parenchyma and recorded ion currents through their plasmalemmata in the whole-cell configuration as well as in membrane patches. We have yet to examine the role and properties of the proton pump in the plasmalemma. Preliminary results of this work were communicated at the 9th International Workshop on Plant Membrane Biology (Monterey, CA, July 19–24, 1992).

[1] L.H.W. was supported by the Studienstiftung des deutschen Volkes, and part of the equipment was acquired through grants from the Deutsche Forschungsgemeinschaft to K.R.

[2] Present address: Werkgroep Fysiologie en Biochemie van Planten, Vrije Universiteit, De Boelelaan 1087, NL1081HV Amsterdam, The Netherlands.

* Corresponding author; fax 49–551–397823.

Abbreviations: E_{rev}, reversal potential; E_X, equilibrium potential of the ion species X; HEEDTA, *N*-hydroxyethyl-ethylenediamine-triacetic acid; Hz, hertz; KIRC, K^+-selective inwardly rectifying conductance; KORC, K^+-selective outwardly rectifying conductance; NORC, nonselective outwardly rectifying cation conductance; pS, picosiemens; TEA^+, tetraethylammonium; U_H, holding potential.

MATERIALS AND METHODS

Cultivation of Plants

Barley plants (*Hordeum vulgare* L. cv Apex; Cebeco Saaten, Celle, Germany) were grown on full-strength Long Ashton nitrate-type solution (Hewitt and Smith, 1975) on a hydroponic substrate (Lecaton light-expanded clay aggregates, Leca Deutschland, Pinneberg, Germany) in a temperature-controlled room at 22/18°C day/night and in light from fluorescent tubes (Osram L65W/25S; quantum flux 300 μmol m^{-2} s^{-1}). The nutrient solution was continuously aerated and replaced every week. Plants were harvested after 3 to 5 weeks.

Properties of Protoplasts from the Xylem Parenchyma

The complex anatomy of the stele (Heimsch, 1951) required a specific method for the isolation of xylem parenchyma cells. The cells of interest were those bordering early metaxylem vessels; these vessels form an outer ring in the stele, alternating with the metaphloem (Fig.1), and are differentiated at 0.3 to 0.4 cm above the root tip (Läuchli et al., 1974). The early metaxylem is presumed to be the most effective longitudinal transport pathway for ions to the shoot (Läuchli et al., 1974). The selective preparation of protoplasts from this tissue was achieved by making use of the lignification pattern in the stele of nodal roots. Figure 2 shows a free-hand cross-section of the stele 1 cm above the root tip. The slice was stained with astra blue and safranine red (indicating lignification). Lignification, as displayed in the center of the stele and, less conspicuously, in the endodermis and the pericycle, slows down cell wall digestion. Figure 3 documents the state of differential cell wall hydrolysis after about 120 min of incubation in the medium used for protoplast preparation. Digestion in the outer ring of xylem vessels was advanced, whereas the center of the stele and the cortex remained unaffected. Time courses were similar in thin sections used for anatomical and histological inspection and in thick sections used for protoplast production. For an unambiguous demonstration of the xylem parenchyma origin of the protoplasts and of the absence of contamination by phloem tissue, isolated steles from the proximal zone of the root (in which only the phloem tissue had remained free from lignification) were subjected to the differential digestion just described. The enzymic treatment led to a complete decomposition of solely the phloem cells. Microscopic inspection showed that the lignified stele remained. The protoplast yield of this tissue was only 1.3% of that obtained with the distal stelar tissue 0.7 to 2 cm above the root tip, which was used as a control. Protoplast yield was determined with a Thoma hemocytometer (W. Schreck, Hofheim/TS, Germany). Contamination with protoplasts from the pericycle cannot be excluded, although the pericycle walls often remained undigested (Fig. 3). The presence of phloem-parenchyma protoplasts was unlikely because this cell type appears not to exist in barley roots (Warmbrodt, 1985); protoplast formation from sieve tubes or companion cells has not yet been reported.

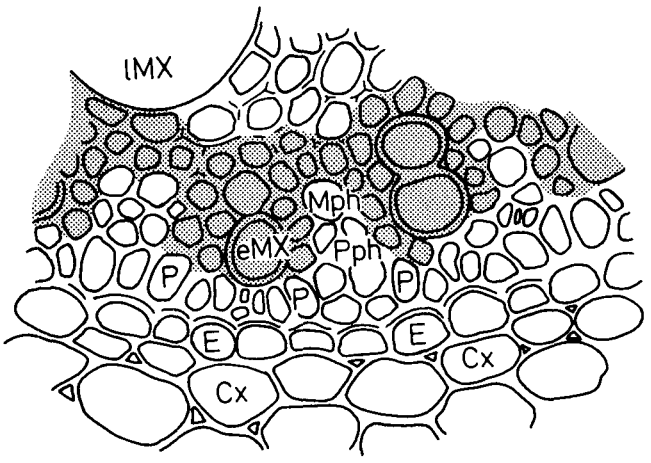

Figure 1. Distribution of tissues in the periphery of the stele. The stippled area marks the region from which early metaxylem protoplasts originated. E, Endodermis; eMX, "early" metaxylem vessel; lMX, "late" metaxylem vessel; Mph, metaphloem (sieve tube); Pph, protophloem (sieve tube); P, pericycle; Cx, cortex.

We elaborated the following routine for protoplast isolation from xylem parenchyma cells. Roots were selected from the first or second node (without lateral root formation and up to a length of about 5 cm). Their tips were removed, and the cortex was stripped by hand. This could readily be performed because the stele was partly lignified. Stelar sections were cut with a razor blade 0.7 to 1.5 cm above the root tip and collected in a Petri dish in 1 mM $CaCl_2$ on ice. After blotting them with tissue paper they were minced to small pieces, which were then transferred to 2% (w/v) cellulase Onozuka R 10 (Yakult Honsha, Tokyo, Japan), 0.02% (w/v) Pectolyase Y-23 (Seishin Pharmaceutical, Tokyo, Japan), 2% BSA (w/v), 10 mM Na ascorbate, and 1 mM $CaCl_2$. The pH was adjusted to 5.5 with H_2SO_4. Mannitol was added to a total osmolality of 500 mOsm, checked with an osmometer (Wescor 5100C, Logan, UT). The digestion proceeded under moderate agitation in a shaking water bath (about 100 excursions per min) for 120 to 150 min at 20°C. The suspension was then filtered through 120- or 200-μm nylon mesh (Züricher Beuteltuchfabrik, Rütlikon, Switzerland) and the residue was rinsed with about 50 mL of 1 mM $CaCl_2$, 500 mM mannitol, thus diluting the preparation about 25-fold and separating the protoplasts from cell wall debris. The suspension was filtered through 80- and 23-μm mesh screens and then centrifuged at 100*g* for 10 min (Minifuge 2, Heraeus Christ, Osterode, Germany). The pellet was resuspended in about 3 mL of the uptake medium and centrifuged again. The supernatant was discarded and the pellet was dispersed in about 100 μL of the uptake medium.

Cell Dimensions

Cell circumferences were determined from photographs of cross-sections of the stele. These were projected on an Apple graphics table (Apple Computer, Cupertino, CA) and evaluated with Apple software. The cell lengths were measured on longitudinal free-hand sections under the microscope using a calibrated ocular micrometer; protoplast diameters

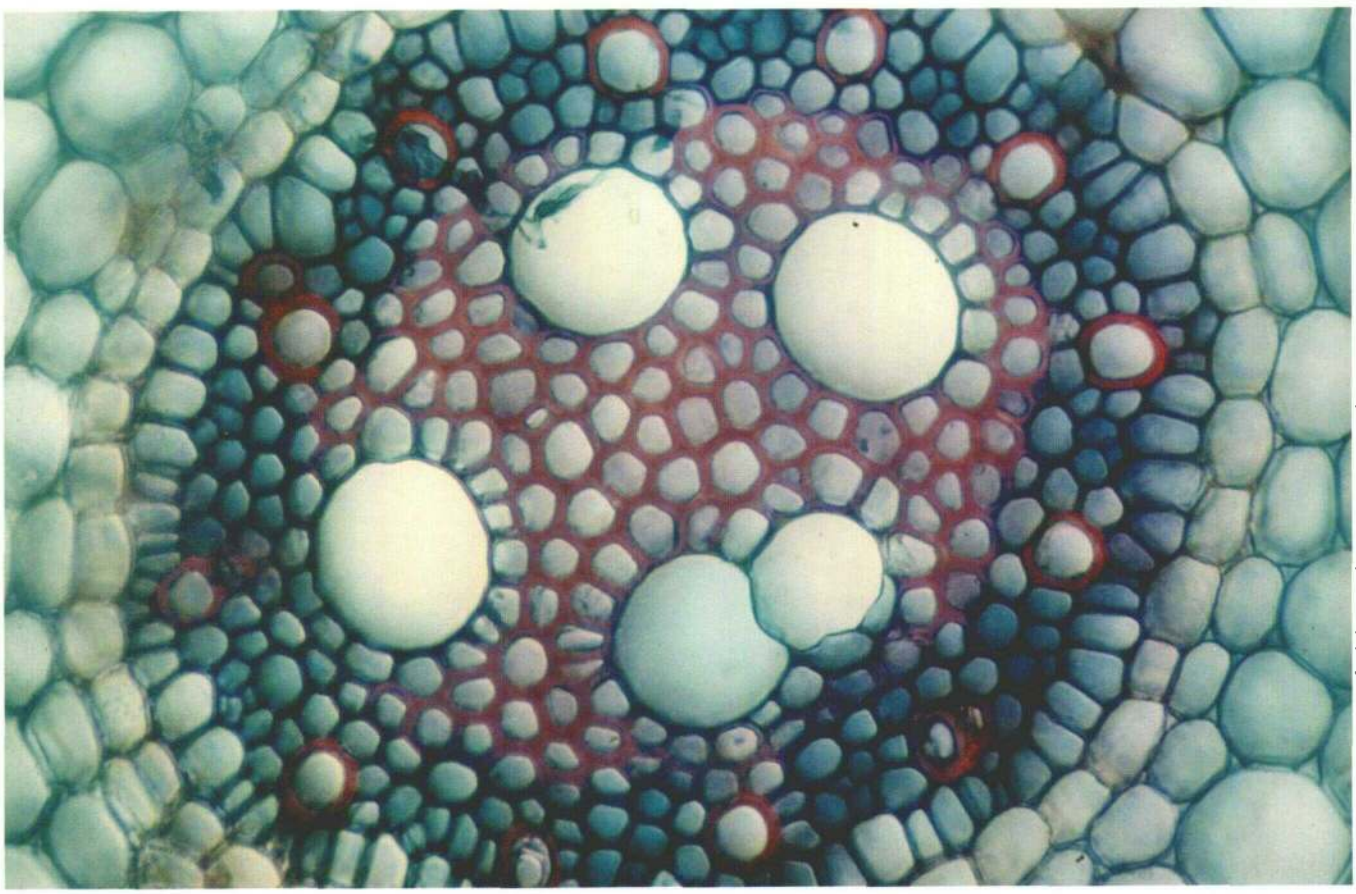

Figure 2. Cross-section of the stele 1 cm above the tip of a nodal root, stained for 10 min in 0.5% (w/v) astra blue and 0.5% (w/v) safranine red, followed by a rinse with water. Red stain indicates lignification.

were determined likewise. Cell volumes and surfaces were calculated assuming a cylindrical shape of the cells.

Electrophysiology

Experiments were performed in the whole-cell and outside-out patch configuration (Hamill et al., 1981). Pipettes were fabricated from borosilicate glass capillaries (Kimax 51, Kimble Products, Vineland, NJ); typically, they had a resistance of 3 to 8 MΩ in the standard solutions for whole-cell experiments and about 15 to 20 MΩ in solutions used to establish the outside-out patch configuration. The reference electrode was connected to the bath via a salt bridge, or, when a solid AgCl pellet was used, it dipped directly into the bath. The use of the pellet electrode was restricted to experiments in which the Cl^- concentration was not to be changed. The potential difference between patch and ground electrodes was compensated after lowering the tip into the bath. Liquid junction potentials were determined according to Neher (1992) and corrected for if the value exceeded ±2 mV. Junction potentials at the bath electrode, resulting from solution changes, were treated likewise. Voltage clamp measurements were made with an EPC 7 patch-clamp amplifier (List Electronic, Darmstadt, Germany). Data were low-pass filtered with an eight-pole Bessel filter (Frequency Devices, Haverhill, MA) at 500 Hz (−3 dB corner frequency), if not stated otherwise, and digitized by an ITC 16 interface (Instrutech, Elmont, NY) with a sampling rate of 2 kHz. For generating pulse protocols and storing and evaluating data, an Atari Mega ST4 computer (Atari, Sunnyvale, CA) was used. Alternatively, data were stored on videotape using a VR-10 interface (Instrutech). Data were analyzed using patch-clamp software from Instrutech.

Solutions

Solution A, in the pipette: 120 mM KCl or potassium glutamate, 10 mM Tris, 10 mM EGTA, 2 mM MgATP, 1.93 mM $MgCl_2$, pH 7.2, adjusted with Mes. The Ca^{2+} concentration was 1 μM, adjusted with calcium gluconate. If potassium glutamate was used, 1 mM $CaCl_2$ was added. The total amount of Ca^{2+} to be added was calculated according to the program "Calcium" (Führ et al., 1993). Modifications of this composition are indicated in the text. Solution B, in the bath: 30 mM KCl or potassium glutamate, 10 mM Hepes, 2 mM $MgCl_2$, 1 mM calcium gluconate or $CaCl_2$ (total Cl^- concentration < 6 mM). Often, increased Ca^{2+} concentrations were applied (10 and 40 mM) using calcium gluconate (see text). The pH was adjusted to 5.8 (Mes). The internal solutions were filtered through 0.22-μm filters. Activity coefficients for

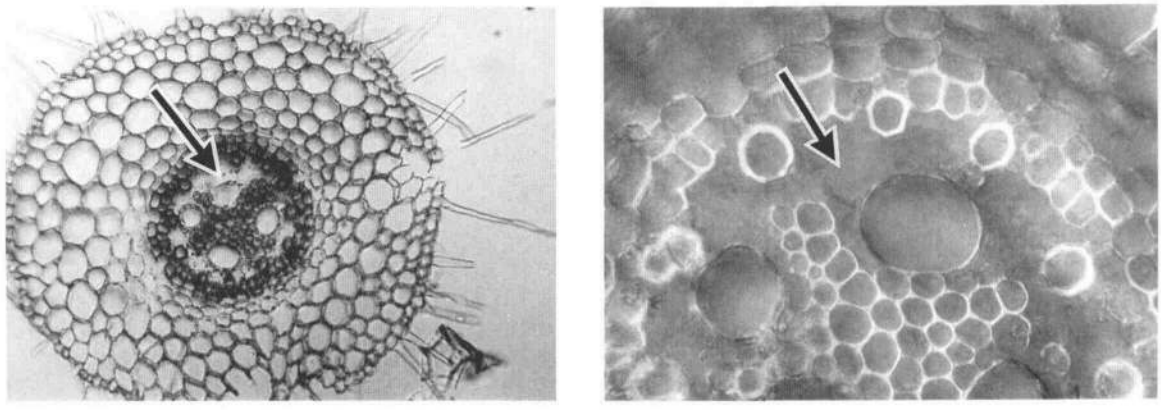

Figure 3. Partly digested cross-section after 120 min of incubation in the enzyme solution used for isolation of protoplasts. Left, Overview; right, detail showing erosion of xylem parenchyma. Arrows indicate advanced cell wall lysis around xylem vessels.

the calculation of reversal potentials were determined according to the Debye-Hückel theory using the equation of Davies (Robinson and Stokes, 1968).

RESULTS

Light Microscopy

The structure of the stele of barley roots was described by Heimsch (1951) and Warmbrodt (1985): The xylem is "discontinuous," meaning that early and late metaxylem vessels are separated by two to three cell layers (Fig. 1). The late metaxylem vessels remain undifferentiated up to 2 cm above the root tip. We apply the term "xylem parenchyma cell" to cells situated around the outer metaxylem elements. These cells have an elongated, almost tube-like shape (Table I). Comparison of the in situ volumes of these cells with those calculated from protoplast diameters leads to the conclusion that each parenchyma cell disintegrated, during the course of isolation, into an average of six protoplasts. These protoplasts possessed a wide, dense cytoplasm and a relatively small vacuole (Fig. 4), whereas in cortical cells, almost the whole volume was occupied by the vacuole. Comparing surfaces of protoplasts, calculated from diameters, with capacitive transients in the whole-cell configuration, the specific capacity of the plasmalemma was determined to have been 0.88 ± 0.10 microfarads cm^{-2} ($n = 10$).

Two Types of Outward Rectifiers

In the whole-cell configuration, voltage pulses starting from −72 mV to more positive values (in increments of 10 mV) caused increases in membrane conductance (Fig. 5). Current densities were calculated from steady-state currents after subtraction of the instantaneous component and plotted as functions of the pulse potentials. If the depolarizing step was followed by a capacitive current spike, notwithstanding the preceding compensation procedure, the current amplitude 5 to 10 ms after the potential jump was taken as the instantaneous component. The presence of two types of outward rectifiers could be recognized; they were distinct with respect to their voltage dependence, kinetics, ion selectivity, and blockage by TEA^+. Based on their voltage dependence and selectivity we assigned to them the acronyms KORC (K^+-selective Outwardly Rectifying Conductance) and NORC (Nonselective Outwardly Rectifying cation Conductance). (We use these abbreviations within this paper merely to condense description. The conductances we found need to be characterized further before they can be assigned their names within a standardized nomenclature still to be agreed upon).

Table I. *Dimensions of xylem parenchyma cells and protoplasts*

	Mean ± SD	*n*
Cell circumference	26.6 ± 6 μm	543
Cell length	328 ± 87 μm	21
Cell volume	18.5 ± 5.7 pL	21
Cell surface	8837 ± 2516 μm^2	21
Protoplast diameter	17.94 ± 6.04 μm	215
Protoplast volume	3.02 ± 1.10 pL	215

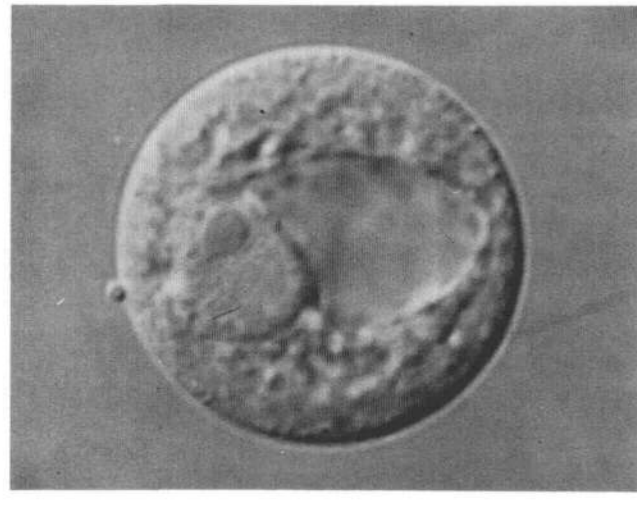

Figure 4. Protoplast from the xylem parenchyma with a sharply contoured vacuole and a wide cytoplasm. See Table I for dimensions.

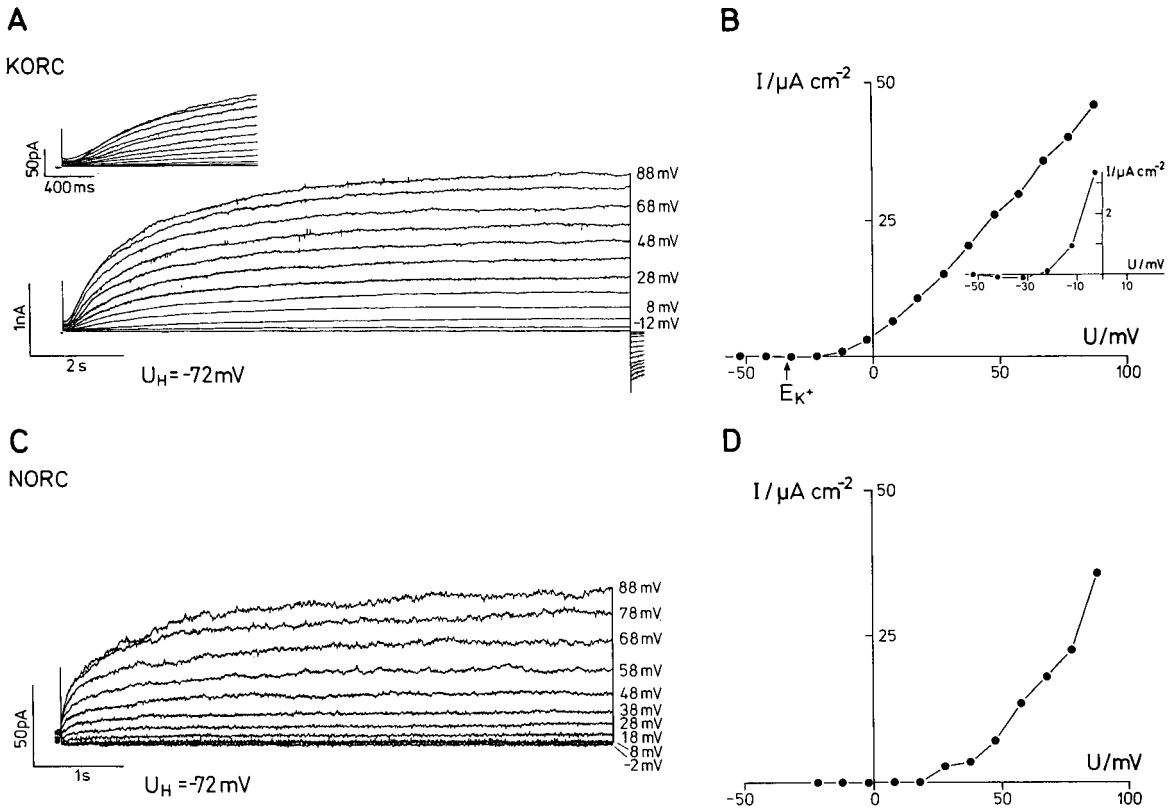

Figure 5. Two types of whole-cell outward currents activated by depolarizations of the plasmalemma. A, Current traces recorded during depolarizing voltage pulses of 12-s duration. Consecutive voltage pulses increased to full decades in increments of 10 mV from a U_H of −72 mV. Between pulses, the membrane was clamped to U_H for 30 s. Activation of KORC occurred; it was characterized by sigmoidal activation kinetics. Inset, First 2 s of the current traces at an expanded time scale). B, Current-voltage relation obtained from the pulse experiment shown in A. Current densities were calculated from steady-state currents after leak subtraction. Inset, Small inward currents at test potentials between −50 and −25 mV, i.e. at voltage < E_{rev}. C, Activation of NORC during 6-s depolarizations. Between stimuli, the membrane was clamped to U_H for 15 s. D, The corresponding current-voltage curve. In both experiments, identical solutions (potassium glutamate) were used with 10 mM Ca^{2+} in the bath. Each set of currents through KORC or NORC represents 10 replications.

Voltage Dependence

One of the rectifiers, KORC, became conducting at membrane potentials above −50 mV. It activated below E_K and passed small inward currents if voltage < E_K (Fig. 5B, inset). Its time course of activation displayed sigmoid kinetics. If the potential was stepped to values more positive than E_K, outward currents appeared that strongly increased with increasing membrane potential (Fig. 5, A and B). This conductance resembled the K^+ outward rectifier that had already been described for a number of cell types from various tissues, including guard cells (see "Discussion"). The other rectifier, NORC, was characterized by activation at potentials above +20 or +40 mV (Fig. 5, C and D). In the majority of protoplasts, either one of the two types of conductances was prevalent, as is demonstrated in Figure 5. Occasionally, both types appeared simultaneously or successively in the same protoplast (Fig. 6).

Selectivity

"Tail" protocols were imposed to investigate the selectivities of the outward rectifiers (Fig. 7). Outward currents were activated during prepulses; repetitive steps to more negative potentials followed in increments of −10 or −20 mV. Instantaneous amplitudes of tail currents were determined by fitting exponential functions to the time courses of deactivation, thus correcting for leak and capacitive currents. In case of incomplete deactivation, leak current was obtained by linear extrapolation and subtracted from the absolute value determined for time zero. Figure 7A shows a tail current experiment performed on KORC (note the S-shaped activation kinetics). Tails reversed close to the equilibrium potential of K^+, indicating that currents were carried mainly by this ion. However, there was a small but significant deviation from E_K. With 120 mM KCl in the pipette and 30 mM KCl in the bath, tails turned at −24 ± 3 mV (n = 5), whereas E_K was calculated to be −34 mV. This deviation was not due to a conductance for Cl^-, because substitution of Cl^- with glutamate (generally considered to permeate membranes only at very low rates) as a counterion for K^+ did not cause a shift in the reversal potential (E_{rev} = −24 ± 2 mV, n = 8). With Ca^{2+} and Mg^{2+} being the only candidates left, it was concluded that divalent cations were able to enter the protoplasts via KORC. Current voltage relations for tail currents were gen-

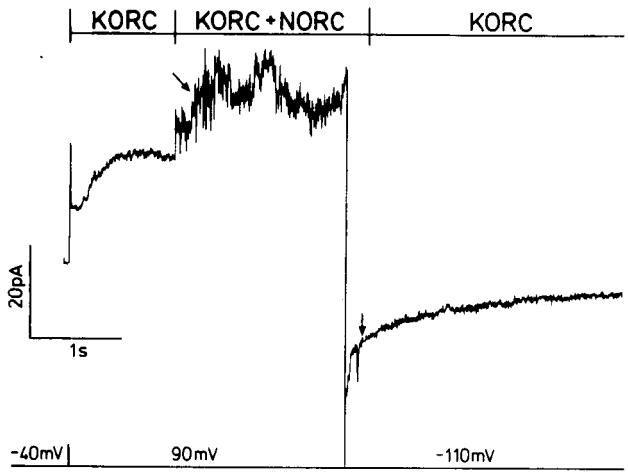

Figure 6. Example of an activation of both types of outward rectifier in a small protoplast by a depolarizing voltage step. Single NORC channel events can be detected (first arrow). Sigmoid kinetics appeared in the KORC current. Note that both types of current deactivated on repolarization (second arrow, at tail current). This protoplast had a capacitance of 3 picofarads, equivalent to a diameter of about 10 μm.

erally asymmetric; inward currents saturated below −50 mV, whereas outward currents were linear up to 90 mV (not shown). This possibly reflects rectifying properties of open channels, such as were also observed for an outwardly rectifying K^+ channel in *Arabidopsis* (Spalding et al., 1992).

A tail experiment performed on NORC is shown in Figure 7C. Tail currents went to zero between 0 and −12 mV. None of the Nernst potentials of the ion species present in the pipette and bath solutions were positioned there. The reversal potential did not depend on the Cl^- activity ratio either (Fig. 7D), indicating that the rectifier involved was selective for cations. To check whether the conductance was preferentially one for Mg^{2+}, as the reversal potential might indicate, the external Mg^{2+} concentration was reduced from 2 mM to 91 μM; this shifted the Mg^{2+} equilibrium potential from 0 to −36 mV. The reversal potential of the tail currents appeared now at −9 ± 5 mV, versus −6 ± 5 mV without a Mg^{2+} gradient (n = 3), implying that Mg^{2+} was not playing a major role either. Hence, currents were carried by K^+ and likely by Ca^{2+} as well.

For a survey of the selectivity for other alkali metal ions, K^+ in the bath was replaced by Na^+, Rb^+, Li^+, or Cs^+ in further tail experiments (not shown). The measured reversal potentials indicated that NORC selected weakly among alkali metal cations, with the exception of Li^+, for which an E_{rev} of −30 mV (versus −6 mV in the other cases, n = 3) indicated reduced permeability. From this set of experiments, the derived selectivity sequence was $Ca^{2+} > K^+ \approx Na^+ \approx Rb^+ \approx Cs^+ > Li^+ > Mg^{2+} > Cl^-$. Admittedly, in experiments with varying external Ca^{2+} concentrations, we failed to show participation of Ca^{2+}. With 40 mM Ca^{2+} in the bath and 1 μM Ca^{2+} in the pipette, E_{rev} was −3.4 ± 2.9 mV (n = 5); with 10 mM/1 μM Ca^{2+} (bath/pipette) it was −6 mV (n = 3), and with 1 mM/1 μM Ca^{2+} it was 0 and −12 mV (n = 2). These contradictory findings may be reconciled if one assumes that Ca^{2+} currents are not affected by shifts in equilibrium potentials if they are close to E_{rev}. This anomaly can occur if channels behave like multi-ion single-file pores (Hille, 1992). The reversal potential method for the determination of relative permeabilities obviously has its limitations.

Kinetics

The time course of current activation was sigmoidal for KORC currents, with half-times between 0.5 and 1.5 s (increasing with decreasing test potential), whereas activations of NORC currents were best described by double-exponential functions, with time constants of about 0.2 and 1.5 s, and they showed no voltage dependence. The decay of KORC currents was single exponential; the time constant varied between 0.3 and 3 s (Fig. 8). Deactivation of NORC currents, on the other hand, was again best described by a sum of two exponentials, although the slow component, being by far the minor one, could not be resolved in all experiments. The major component of the NORC currents deactivated significantly faster than the KORC currents, thus providing a further means to discriminate between the currents.

Blockage by TEA^+

The K^+ channel blocker TEA^+ (Bentrup, 1990; Tester, 1990; Hille, 1992), at a concentration of 20 mM in the bath reduced KORC currents by 80 to 90% within 2 min. The block was not voltage dependent (Fig. 9) and was reversible (not shown). Preliminary data indicate that the same effect could be obtained with a far lower concentration (0.5 mM), although it was very slow (L.H. Wegner and A.H. De Boer, unpublished data). In contrast, NORC currents remained unaffected, even with a TEA^+ concentration as high as 20 mM. This differential effect of a channel blocker might offer a tool in segregating activities of KORC and NORC.

Single-Channel Recordings

In two experiments, single-channel events were recorded in the outside-out configuration. Under symmetrical conditions with respect to K^+ (100 mM potassium gluconate), a unitary conductance of 21 pS was determined (data not shown). It was not possible to relate it to currents through KORC or NORC in the whole-cell configuration.

An Inward K^+ Rectifier

Hyperpolarizing voltage steps from a holding potential of −33 mV in the whole-cell configuration gave rise to large inward currents (Fig. 10). The "activation potential," i.e. the potential below which these inward currents could be detected, was about −110 mV. Tail experiments disclosed that these were K^+ currents (Fig. 11). Instantaneous current voltage curves of the tails were linear; the strong voltage dependence of the currents was therefore likely due to the gating of channels. In some cases, saturation was observed at positive potentials, as was reported for a similar type of current in mesophyll protoplasts from *Avena* (Kourie and Goldsmith, 1992). However, this may have been an artifact resulting from decreasing deactivation time constants (2–4 ms).

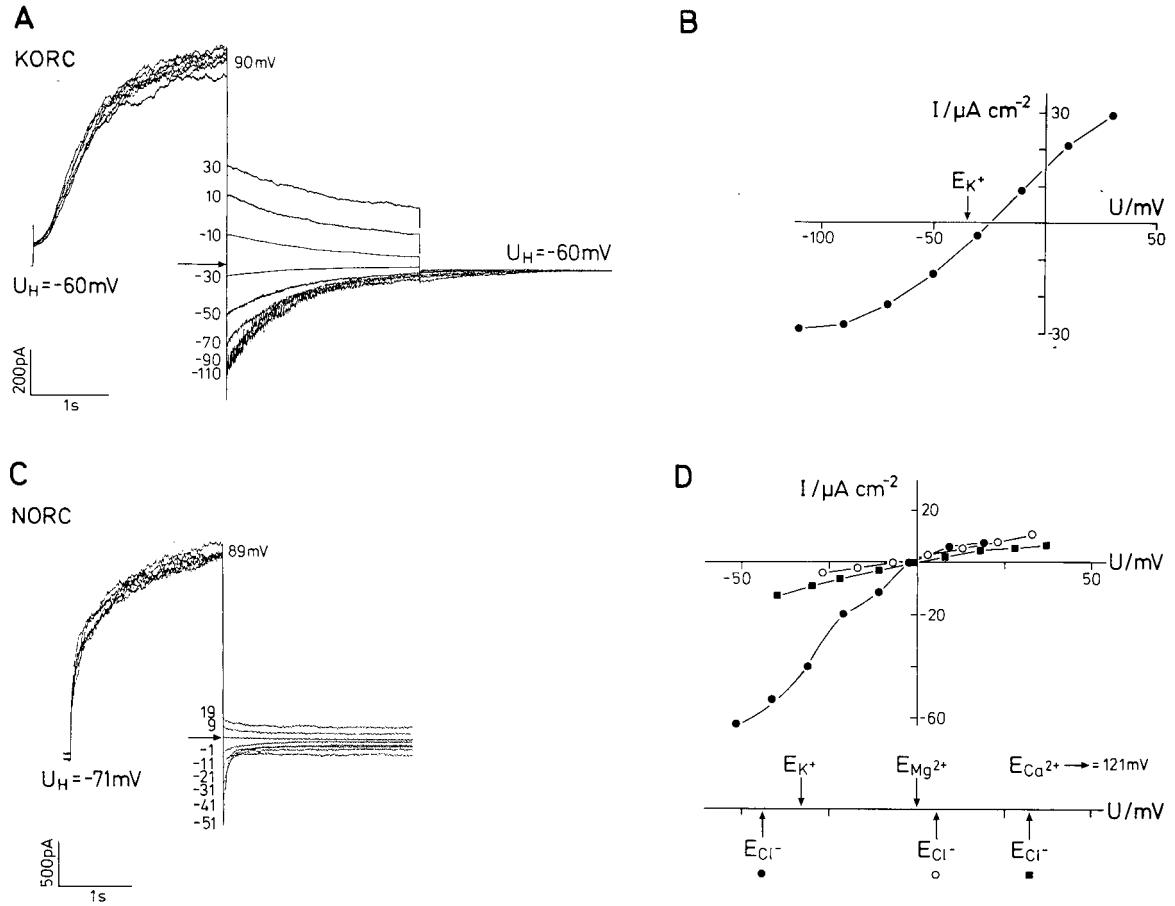

Figure 7. A, Currents through KORC, resulting from a tail protocol with 20-mV step changes in the deactivation potential. Between sweeps, the potential was kept at −60 mV for 10 s. B, By plotting the instantaneous current densities against the potential of the second, deactivation step, a reversal potential of −26 mV was determined by interpolation (E_K = −34 mV). Solutions A and B (KCl) with 10 mM Ca^{2+} in the bath. C, Tail currents through NORC. Double voltage pulses were applied at intervals of 15 s. Pipette, solution A (glutamate); bath, solution B (Cl^-), but 40 mM calcium gluconate. D, Current-voltage relationships obtained with three combinations of Cl^- concentrations in pipette and bath demonstrate that variation of Cl^- gradients across the plasmalemma did not affect the reversal potential of NORC currents. Instantaneous tail currents were plotted against voltage (arrows indicate the three equilibrium potentials of Cl^-). Concentrations of K^+, Ca^{2+}, and Mg^{2+} were kept constant in pipette/bath solutions (120 mM/30 mM K^+, 1 µM/40 mM Ca^{2+}, 2 mM/2 mM Mg^{2+}). Glutamate and gluconate concentrations were varied to substitute for Cl^-. Each experiment was performed at least twice. The determined reversal potentials were: ●, −2 mV; ○, −6 mV; ■, −1 mV. ●, Experiment shown in C. Note the different current scales. Chloride activity ratios (pipette/bath) and the corresponding equilibrium potentials for Cl^- (in parentheses) were 94.2/25.5 (33 mV), 94.2/84.5 (2 mV), and 4.6/25.5 (−44 mV), respectively.

In outside-out patches, channel activity was elicited by hyperpolarization below about −110 mV, although there was a probability of opening also above this potential (Fig. 12, trace recorded at −80 mV). The pattern of channel activity included spike-like events that resulted from simultaneous activation of several channels (one example from 10 recordings). Often, current transitions between distinct channel levels could not be resolved at peak activity. From the events that were discernible, a main conductance level of about 30 pS was determined. Data obtained under symmetrical conditions with respect to K^+ (100 mM) could be fitted with a linear current-voltage relation that passed through the origin. With 30 mM K^+ in the bath and 120 mM K^+ in the pipette, the curve shifted by about 40 mV in the hyperpolarizing direction, in agreement with the displacement in E_K; the currents were K^+ currents. Note that the conductance did not depend on the substrate concentration in this range. The findings that the channel was selective for K^+ and that channel activity strongly increased with hyperpolarization of the membrane below −80 mV may serve as prima facie evidence that the inward K^+ currents recorded in the whole-cell configuration were manifestations of the activity of K^+ inward channels.

Selectivity of the Inward Rectifier for Alkali Ions

Discrimination of K^+ channels against Na^+ is a property of particular interest in the study of root cells, because different mechanisms for the avoidance of salinity stress may be based on the ability of transport proteins to distinguish between

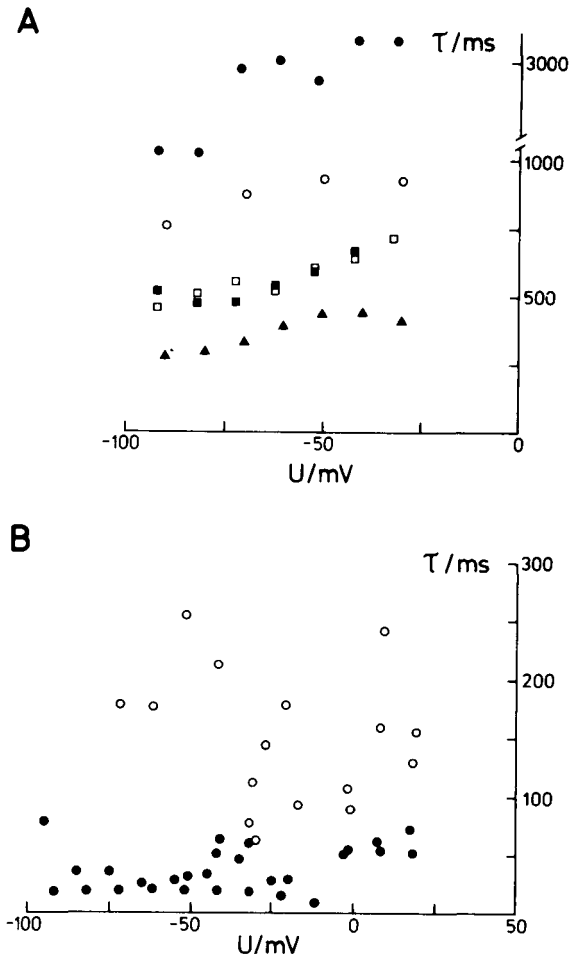

Figure 8. Kinetics of whole-cell outward currents. A, Time constants of the deactivation of KORC currents (Fig. 7) in relation to the tail potentials (from nonlinear least-square fits to the time courses); variability among five individual protoplasts (different symbols). B, Time constants of the fast (●) and the slow (○) component of NORC current deactivation (five experiments) in relation to the tail potentials (from experiments like the one shown in Fig. 7). In two experiments, values up to 600 ms were determined for the slow time constant. Solutions A and B, with 10 mM Ca^{2+} in the bath.

these two ions (Maathuis and Prins, 1990; Schachtman et al., 1991). The alkali-ion selectivity of the inward rectifier in xylem parenchyma cells was examined by recording tail currents under asymmetrical bi-ionic conditions. Double-pulse protocols were imposed on xylem parenchyma protoplasts with 30 mM KCl (or potassium glutamate) in the bath (control) and again after perfusion with a medium in which K^+ was replaced by another alkali ion. Inward currents activated by the prepulse were necessarily carried by the monovalent cation applied externally; thus, the ability of the inward rectifier to transport this cation was already demonstrated by the activation of an inward current per se. From reversal potentials of tail currents (Table II), relative permeabilities for K^+ were calculated using a rearranged form of the Goldman equation (Schroeder, 1988). The following selectivity sequence was obtained: $K^+ > Rb^+ \approx Cs^+ > Li^+ \approx Na^+$.

For an appropriate interpretation of the data, the current-voltage relations of instantaneous tail currents have to be considered as well (Fig. 13). They reflect the voltage dependence of the current passing through the ensemble of open channels in the whole-cell configuration. Thus, only interactions of the permeating cations with the channel pore are reflected, whereas a modification of gating does not affect the shape of the current-voltage curve. A comparison of instantaneous current-voltage relationships under bi-ionic conditions clearly demonstrates that the constant-field equation of independent ion movement was not obeyed; the validity of the Goldman equation is restricted, and permeability ratios should not be applied to ion fluxes in situations away from equilibrium.

Apparent irregularities appeared with Rb^+ in the external solution; the curve bent sharply at voltages above the reversal potential and, when normalized with respect to K^+ currents

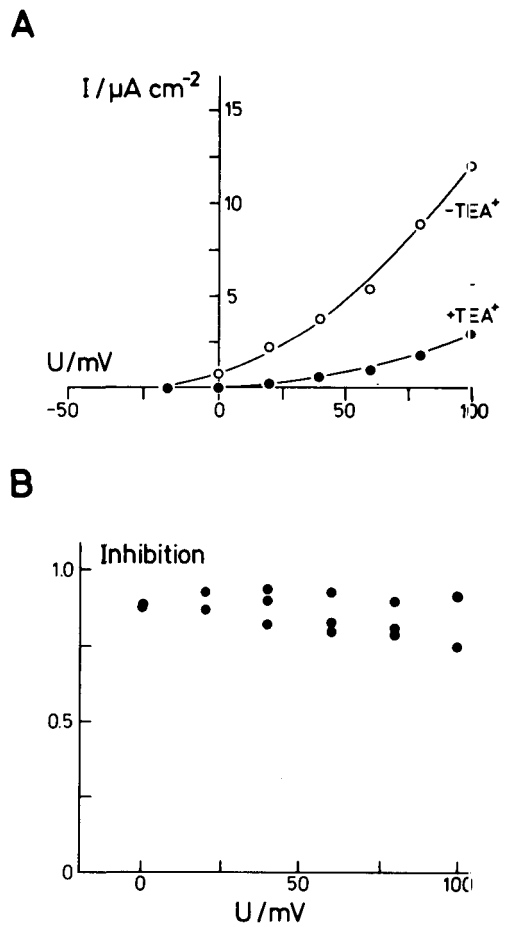

Figure 9. Effect of TEA^+ on KORC whole-cell currents. A, Current densities plotted as functions of the pulse potential with and without 20 mM TEA^+ in the bath. Protocols to test the effect of the blocker were imposed (as shown in Fig. 5) approximately 2 min after perfusion of the bath was completed. B, Voltage dependence of the TEA^+ effect (three examples). Inhibition = $(I_{control} - I_{TEA})/(I_{control})$, where I is current.

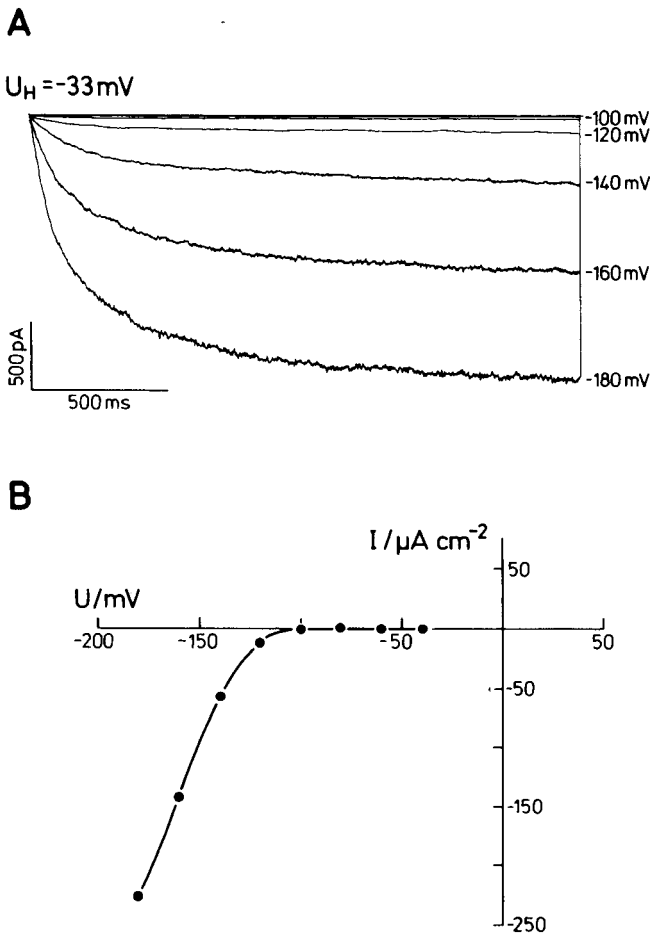

Figure 10. A, Activation of inward currents by negative-going voltage pulses in the whole-cell configuration. From the holding potential at E_K (−33 mV), the membrane was hyperpolarized to potentials shown on the right of each trace. Between consecutive sweeps, the cell was clamped to the holding potential for 5 s. B, The corresponding current-voltage curve (after leak subtraction); solutions A and B (KCl; 1 mM $CaCl_2$ in the bath). The experiment shown represents 20 replications.

in the control, the slope conductance of Rb^+ inward currents was smaller than that for Li^+ (Fig. 13, A and C), although the opposite would have been predicted from the determinations of relative permeabilities. The slope conductance for outward tail currents, carried by K^+, remained unaffected, indicating that the anomaly was not due to a modulation of the open probability of channels by Rb^+ or Li^+.

Replacement of the external K^+ by Na^+ (Fig. 13D) considerably reduced the instantaneous whole-cell conductance over the whole voltage range, either because of a reduction of the open probability of the channel by Na^+, caused by modulation of gating, or because of tight binding of Na^+ in the pore that is not relieved within the short time (4–6 ms) of tail current deactivation.

Surprisingly, inward K^+ channels in xylem parenchyma cells showed a considerable permeability for Cs^+, in contrast to guard cells (Schroeder 1988). Indeed, Cs^+ seemed not to affect the voltage dependence of whole-cell inward currents (not shown).

A "Slow" Anion Channel

Figure 14 shows current traces at various potentials in which channel activity manifested itself with a mean open time of about 1 s. Although the experiment was performed in the whole-cell configuration, single-channel events could be resolved, implying a low channel density or a low open probability or both simultaneously. Current amplitudes are plotted against voltage on the right. The reversal potential extrapolated to a value close to the Nernst potential of Cl^-, disclosing that this anion was the main carrier of the current. The unitary conductance in this case was 46 pS.

In another set of experiments, a higher conductance was determined by imposing voltage ramp experiments on the open channel (Fig. 15). To correct for the background conductance in the whole-cell configuration, currents elicited by the ramp protocol at the closed level of the channels were subtracted (see Tyerman and Findlay, 1989). The holding potential in these experiments was positioned close to the reversal potential of K^+ (−30 mV) to minimize interference by cation transport. Ramps extended from −100 to +75 mV and were applied at intervals of 1 s. The slope was 3 V s^{-1}. With 120 mM KCl in the pipette (and 10 μM free Ca^{2+}) and

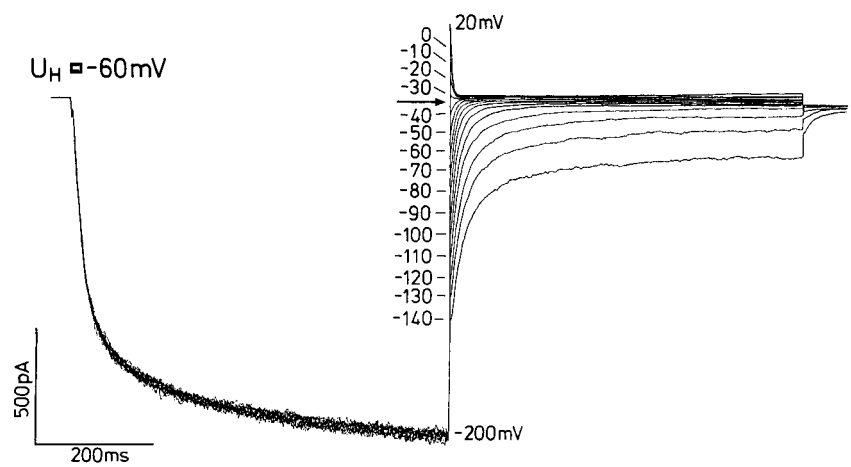

Figure 11. KIRC. After activation at a potential of −200 mV, voltage pulses were applied in decrements of 10 mV. Deactivation of currents was recorded at potentials specified on the left of each trace. For the current-voltage relations of the instantaneous tail currents, see Figure 13A, control with K^+ in the bath. Solutions were as for Figure 10.

30 mM KCl and 40 mM calcium gluconate in the bath, the reversal potential after leak subtraction was 26 ± 3 mV (n = 10; E_{Cl} = 37 mV). The single-channel conductance was 85 and 82 pS (n = 4). Assuming that the deviation of the reversal potential from E_{Cl} was due solely to K^+, a permeability ratio (P_{Cl}/P_K) of 3.2 was estimated.

To prove unambiguously that Cl^- was the main ion carrying these currents, the external Cl^- concentration was elevated to nearly symmetrical conditions (E_{Cl} = 2 mV) while the K^+, Ca^{2+}, and Mg^{2+} gradients were left unchanged. The reversal potential shifted (after correcting for liquid junction potential changes) to 0.12 ± 3 mV (n = 9). Under these conditions (external Cl^- concentration = 114 mM), the single-channel conductance was 77 ± 10 pS (n = 7).

Table II. *Selectivity for alkali metal ions of the KIRC*

Reversal potentials were determined by tail protocols (Fig. 13) after replacement of K^+ in the bath by other alkali metal ions (30 mM; with 120 mM K^+ in the pipette).

Experiment Number	Na^+	Rb^+	Li^+		Cs^+
			E_{rev}		
			mV		
1	−84	−62	−73		−11[a]
2	−69	−53	−68	−60	
3	−71	−51		−58	
4	−68	−58		−57	
			P_x/P_K[b]		
Mean values	0.20	0.41	0.23	0.39	0.43

[a] 120 mM Cs^+ in the pipette, 30 mM K^+ in the bath. [b] P_x/P_K = exp ($-E_{rev}F/RT$), where F = Faraday's constant, R = gas constant, and T = absolute temperature.

DISCUSSION

Comments on the Isolation Procedure

Published procedures for the isolation of protoplasts from roots (Schachtman et al., 1991; Vogelzang and Prins, 1992) refer to root tissue in general, and most protoplasts obtained were presumed to have come from the cortex. Our procedure exploited the lignification pattern in the stele during a differentiating digestion and resulted in a protoplast suspension of certain tissue origin. Artifacts, resulting from protease activity during incubation, were considered minimal, because contamination of the enzyme mixtures with proteases was found to have been low, and BSA, added at a high final concentration (2%, w/v) to the incubation medium, was effective in shielding other proteins against proteolytic activity (W. Diekmann and D.G. Robinson, personal communication). Another matter of concern was the disintegration of the originally cylindrical xylem parenchyma cells into several protoplasts (usually about six). However, most of these subprotoplasts proved to be viable. They were able to accumulate neutral red in the vacuole. While selecting protoplasts for patch-clamp experiments, cytoplasmic streaming was considered an indicator of an intact cytoskeleton and undisturbed energy metabolism.

Ion Channels in the Plasmalemma of Xylem Parenchyma Cells

The outward K^+ rectifier (KORC; Fig. 5, A and B) has counterparts in a variety of species and tissues, including

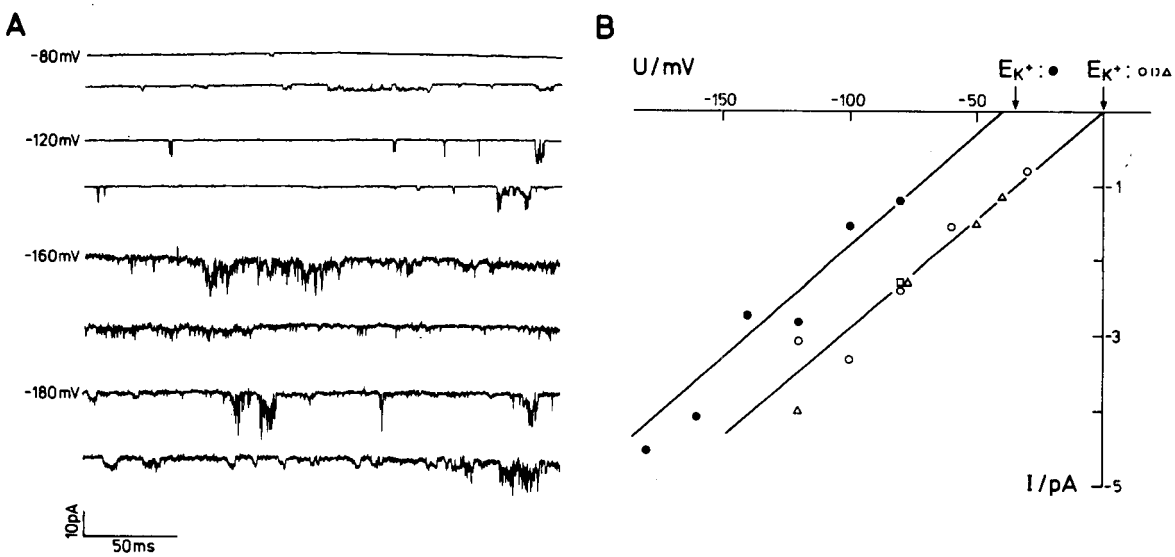

Figure 12. A, Inward single-channel currents recorded in the outside-out configuration. Data filtered at 2 kHz. Because of bursts, single-channel events could be resolved only in parts of the traces. From these segments one main conductance level, corresponding to a K^+-selective channel, could be extracted (see B, solid symbols). Solution in the pipette: 120 mM KCl, 10.9 mM $MgCl_2$, 2 mM MgATP (2 mM free Mg^{2+}), 10 mM HEEDTA, 10 mM Tris, 0.01 mM free Ca^{2+} (gluconate). In another set of experiments (open symbols, n = 3), solutions were 100 mM potassium gluconate, symmetrical, and 5 mM $CaCl_2$ in the bath and 1 μM free Ca^{2+} in the pipette.

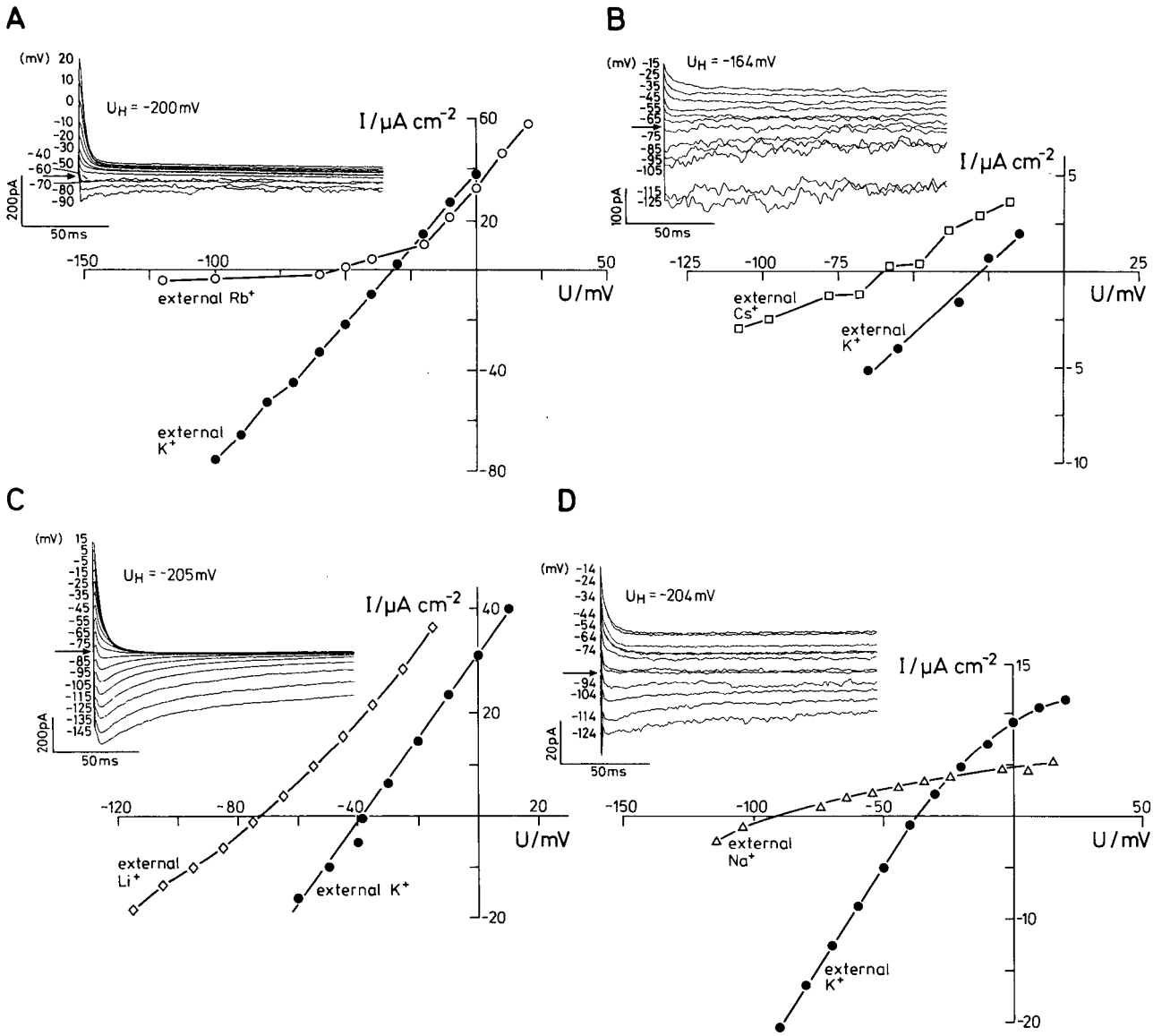

Figure 13. Selectivity of KIRC. Current-voltage relationships of instantaneous tail currents prior to (solid symbols) and after (open symbols) exchanging K^+ in the bath for other alkali metal ions. A, Rb^+; B, Cs^+; C, Li^+; D, Na^+. Note different current scales. Solutions A and B (Cl^- or glutamate); Ca^{2+} in the bath was kept at 10 mM. The insets show recordings of tail currents obtained under bi-ionic conditions; U_H, potential of the activating pulse.

guard cells (Schroeder et al., 1987; Fairley-Grenot and Assmann, 1992), motor cells from pulvini of *Samanea* (Moran et al., 1988), root cells from wheat (Schachtman et al., 1991), cells from cotyledons of *Amaranthus* (Terry et al., 1991), and tissue culture cells from *Arabidopsis* (Cerana and Colombo, 1992), from corn roots (Ketchum et al., 1989), and from tobacco (van Duijn et al., 1993). This channel type may be ubiquitous in cells of higher plants (Hedrich and Schroeder, 1989). Voltage dependence and selectivity (Fig. 7, A and B) of KORC in general agree with the cited literature. The other type of outward rectifier found in xylem parenchyma cells of barley roots (Fig. 5, C and D) was observed recently in xylem parenchyma cells from the mesocotyl of maize (P. Giesberg and A.H. De Boer, personal communication). The NORC was nonselective among cations and not permeated by anions (Fig. 7). Under our experimental conditions, it was activated at positive membrane potentials. A similar type of nonselective cation conductance was discovered in endosperm plasma membrane (Stoeckel and Takeda, 1989).

Remarkably, an inward K^+ current appeared in the whole-cell configuration. A rectifier with similar voltage dependence has previously been reported for guard cells (compare Fig. 10 with the current-voltage relations of Schroeder et al., 1987) and for mesophyll cells (Kourie and Goldsmith, 1992). The inward rectifier of the xylem parenchyma cells was much more permeable for Cs^+ (Fig. 13, Table II) than that described for guard cells (Schroeder, 1988). The selectivity sequence determined for xylem parenchyma cells is in accordance with

the Eisenman sequence IV, indicating moderate interaction with the electric field within the channel pore (Eisenman and Horn, 1983). This observation has bearing on the topology of the pore, which seems to be different in guard cells and xylem parenchyma cells. The shape of the curve for externally applied Rb^+ (Fig. 13A) can be qualitatively explained by a strong, voltage-dependent interaction of this ion with one or, more likely, several binding sites in the pore. Binding reduces the mobility of the ion, thus simulating a block of the channel. With depolarization, Rb^+ is instantaneously expelled from the pore by K^+, which enters from the inside.

Anion channel activity manifested itself in the whole-cell configuration. Gating was "slow," with a mean open time of about 1 s (Fig. 14). Similar recordings have been obtained from the plasmalemma of guard cells (Linder and Raschke, 1992). These authors demonstrated the activity of a "slow anion channel" in outside-out patches and slowly activating anion currents in the whole-cell configuration.

Subpopulations of Protoplasts in Whole-Cell Experiments

In about 10% of the protoplasts tested, delayed increases or decreases of currents did not occur in response to hyperpolarizing or depolarizing voltage pulses; these would have indicated activations or deactivations of rectifiers in the plasmalemma. Currents passed by inward K^+ rectifiers were recorded upon hyperpolarization in about 70% of the protoplasts. The K^+-selective outward rectifier appeared in less than 50% of the protoplasts, as did the nonselective rectifier. We already mentioned the low likelihood of damage to plasmalemma proteins during protoplast isolation; it is equally unlikely that damage caused this heterogeneity. Possibly, differing responses of protoplasts to voltage stimuli were caused by the heterogeneity of the cell fragments we obtained during protoplast production. We believe that, in anatomical terms, the origin of our protoplasts is certain. This provides no guarantee, though, that these xylem parenchyma cells were physiologically alike. In some species, transfer cells have been identified adjacent to the xylem vessels (Kramer, 1983). No obvious specializations in wall morphology were seen in barley roots (Läuchli et al., 1974; Warmbrodt, 1985), but this does not preclude that cells were functionally different.

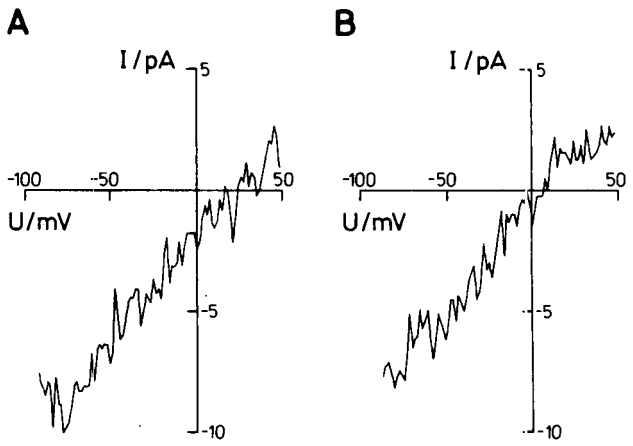

Figure 15. Two voltage ramp experiments on a slow anion channel in the whole-cell configuration (for details of the experimental procedure, see the text). A, Currents elicited by a ramp protocol while one channel was open, with 124 mM Cl^- in the pipette and 34 mM Cl^- in the bath. The reversal potential for this experiment was 25 mV and the slope conductance was 85 pS. B, After raising the Cl^- concentration in the bath to 114 mM, the current-voltage curve shifted along the voltage axis, following E_{Cl} (E_{rev} = 2 mV). The slope conductance was now 82 pS. Data were filtered at 500 Hz.

Salt Release from Xylem Parenchyma Cells: A Hypothesis

Xylem parenchyma cells release salt, taken up by the root cortex, into the water moving toward the shoot. Mechanisms of salt release from plant cells have been studied most exten-

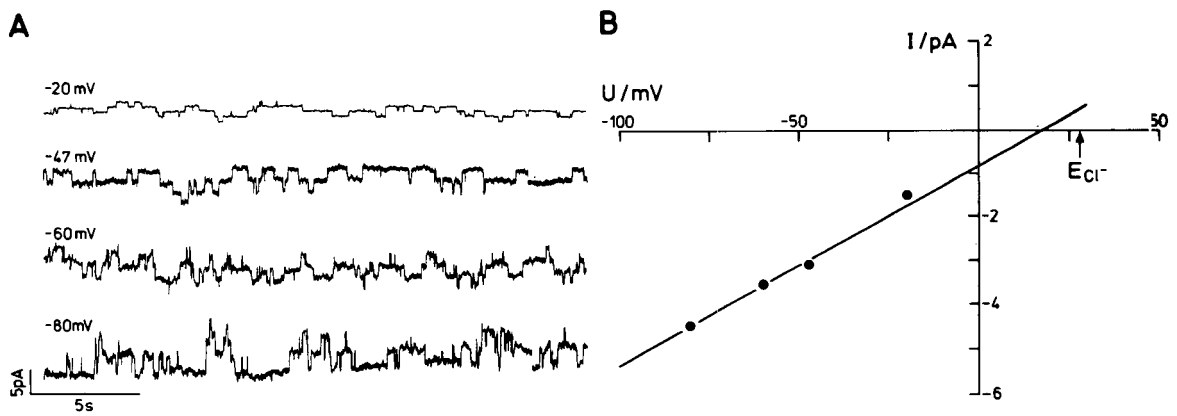

Figure 14. Anion channel. A, Single-channel activities recorded in the whole-cell configuration. Note that the time bar represents 5 s. Solution in the pipette: 120 mM CsCl, 13 mM $MgCl_2$, 10 mM HEEDTA, 10 mM Tris, 2 mM MgATP, pH 7.2, 5 μM free Ca^{2+} (gluconate), osmolality = 530 mOsm (mannitol). Solution in the bath: 30 mM CsCl, 2 mM $MgCl_2$, 1 mM $CaCl_2$, pH 5.8, osmolality = 500 mOsm (mannitol). B, Current-voltage relation for single-channel current transitions, obtained from this experiment; slope corresponds to a conductance of 46 pS.

sively in guard cells. Potassium and anion channels were discovered in the plasmalemma, and they are available as pathways for salt efflux during stomatal closure (citations in the introduction). Our observations on whole-cell currents and single-channel activities in the plasmalemma of xylem parenchyma cells appear to confirm our initial supposition that in roots a similar mechanism of simultaneous release of anions and cations through channels into the apoplast would bring about salt transport into the apoplast of the xylem (Fig. 16). In the whole-cell patch configuration, K^+ currents similar to those found in guard cells were recorded as the membrane was depolarized (Fig. 5, in comparison with Schroeder et al., 1987). This conductance (KORC) could serve as a pathway for K^+ efflux to the xylem sap. However, continuing electroneutral salt flow requires a permeability for anions at potentials positive of E_K. We observed anion channel activity in whole-cell experiments in the required voltage range (Fig. 14). A rough estimate of macroscopic ion fluxes, calculated from the measured channel densities and activities, fell short of the experimental data for Cl^- fluxes presented by Pitman (1971). More recently, B. Köhler (unpublished results) has acquired and evaluated new recordings of anion channel activities in xylem parenchyma protoplasts. She arrived at products of channel density, n (cm^{-2}), and open probability, p, that were 4 to 40 times larger than our initial estimation, and the estimated anion conductance exceeded by far the requirement for passive Cl^- flux into the xylem vessels. Two other observations were also consistent with the hypothesis of passive salt release. The first is that KORC showed a significant permeability for Na^+; it could be as high as that for K^+ (our unpublished data). Barley is known to be moderately salt tolerant and to take Na^+ into the shoot. The second is that the physiologically relevant ion, NO_3^-, can pass through the slow anion channel, which is about as permeable for NO_3^- as for Cl^- (our unpublished data).

Activity of NORC appeared only at positive membrane potentials. We suggest that it serves as a protection mechanism, preventing the membrane potential from shifting to potentials more positive than about 30 mV. Voltages in this range, generally considered unphysiological, could occur if the anion permeability of the plasmalemma exceeds that for cations at large anion gradients into the apoplast.

Passive salt release requires negative electrochemical potential gradients for the anions and cations to be transferred and is restricted to a limited range of membrane potentials in which channels for anions and cations are active simultaneously. Direction and magnitudes of chemical potential gradients in roots can be derived from the composition of the exudate of excised roots. The review by Anderson (1976) summarizes the findings that concentrations of K^+ and Cl^- were between 20 and 30 mM. Assuming the cytoplasmic concentration of K^+ to be about 100 mM (see Dunlop and

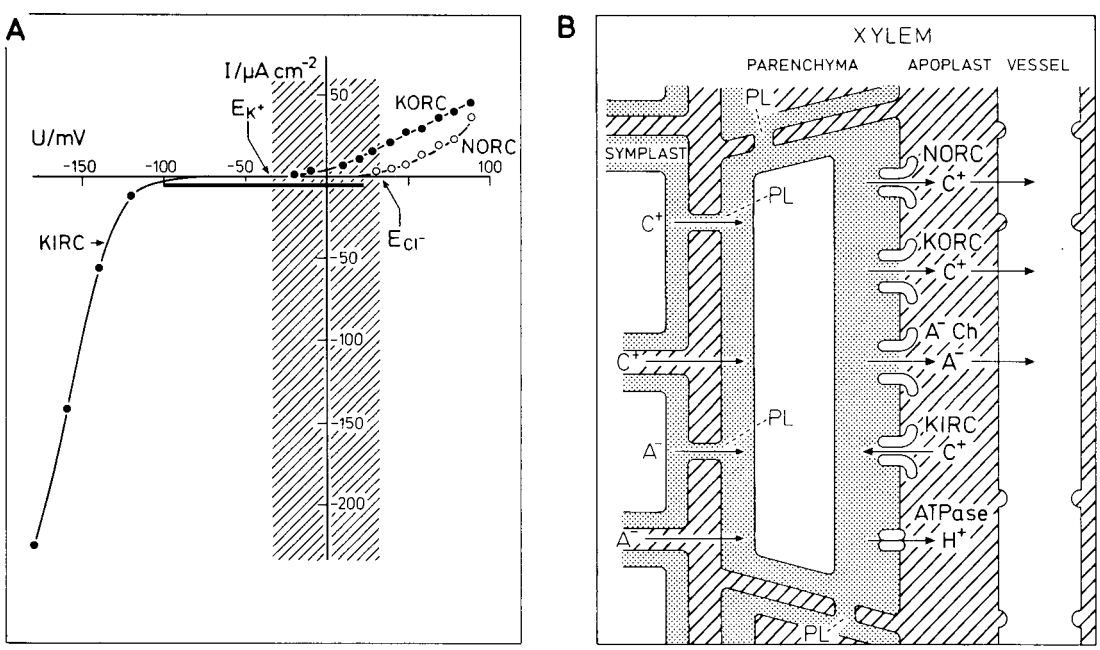

Figure 16. A, Schematic current-voltage plot, summarizing the electrical properties of the plasmalemma of xylem parenchyma cells in barley roots. Ion gradients used to calculate equilibrium potentials correspond to the standard concentrations of the whole-cell experiments (see "Materials and Methods") and are supposed to reflect physiological conditions under root pressure (although, for simplification, only K^+ and Cl^- are considered). Salt efflux from xylem parenchyma cells, i.e. simultaneous movement of anions and cations through channels in the plasmalemma, will follow electrochemical gradients of the ions involved in the range of potentials indicated by shading. Anion channel activity was observed in the voltage range indicated by the solid bar. B, A simplified anatomy of ion paths from the root symplast (stippled) into the apoplast of the stele (hatched) and into xylem vessels. In parallel, apoplastic transport can occur. The locations of the transport proteins in the plasmalemma of xylem parenchyma cells need not be vectorially oriented but very likely are distributed around the cell. A^-, Anion; A^-Ch, anion channel; C^+, cation; PL, plasmodesma.

Bowling [1971a], who claim, however, to have measured vacuolar concentrations), an ion gradient allowing passive release of ions could be maintained even when exudation proceeds. In transpiring plants, the gradient would be about 10 times steeper (Pitman, 1982). Turning to the membrane potential of xylem parenchyma cells, salt efflux would require a potential positive of E_K (Fig. 16A), similar to that in guard cells exposed to ABA (Thiel et al., 1992). Some relevant values have been reported by Dunlop (1982) and Walker and Graham (1987). In *Trifolium* and *Lolium* seedlings, potential differences between the xylem parenchyma cells and adjacent xylem vessels were shown to range from −79 to −100 mV (inside the cell negative). In the latter report, which deals with rye roots, a potential difference of about −50 mV was obtained. Unfortunately, no information on the ionic relations was given, and no equilibrium potentials can be estimated. However, these values are in the range of the depolarized state found by Thiel et al. (1992) for guard cells. The significance of the electrochemical potential difference of ions between xylem parenchyma cells and the xylem sap for understanding the transport mechanism was fully recognized by Dunlop and Bowling (1971b) in their work on maize roots. These authors calculated negative values for both K^+ and Cl^-, indicating that "loading" was thermodynamically passive.

Another piece of evidence supporting our hypothesis comes from the observation that perfusing the stele with fusicoccin strongly reduced the transport of K^+ to the xylem sap (De Boer, 1985; Clarkson and Hanson, 1986). Fusicoccin is known to stimulate proton pumps (Marrè, 1979), and thereby to hyperpolarize the plasmalemma. This finding is in agreement with salt release through channels, but not with the chemiosmotic scheme that was suggested by Hanson (1978).

Development of root pressure is compatible with passive salt release into the xylem after salt uptake by the cortex. There is a symplastic continuum extending from the rhizodermis to the xylem parenchyma cells, allowing ions to diffuse passively to the sites of release (Clarkson, 1989). A salt concentration of 20 mM in the xylem, resulting from salt loss from the parenchyma, would correspond to a water potential of −1 bar and suffice for water uptake into the root if the water potential in the soil was greater than −1 bar.

Although the hypothesis of passive salt release into the xylem is consistent with the results of our patch-clamp study and with reported observations on whole roots, we are aware that our view of radial ion translocation in roots may be oversimplified and that an analogy to the transient efflux of salts from guard cells has its limitations, because it neglects tissue-specific aspects of transport. There is a symplastic continuum extending from the rhizodermis to the xylem parenchyma cells, allowing ions to diffuse passively to the site of release (Clarkson, 1989). Conflicting data come from measurements of radial K^+ gradients with the electron probe microanalyzer, showing K^+ accumulation in stelar parenchyma tissue (Läuchli et al., 1971). This finding may be related to an uptake system for K^+ in the plasmalemma of these cells (Fig. 10). Uptake of K^+ from the apoplast would require hyperpolarization. Indeed, the presence and activity of proton pumps has been shown with different techniques (De Boer and Prins, 1985; Clarkson and Hanson, 1986; Parets-Soler et al., 1990; Cowan et al., 1993), and evidence for H^+ pump currents in xylem parenchyma cells has been found in recent recordings of B. Köhler (unpublished data).

An interpretation of the presence of mechanisms for ion loss as well as uptake in the plasmalemma of xylem parenchyma cells will have to take into account the large contact surface between symplast and apoplast in the stele. There may be spatial as well as temporal patterns of hyperpolarized and depolarized states within the cells of the xylem parenchyma (and among them) forming an intricate mechanism of cooperation between salt accumulation and discharge.

ACKNOWLEDGMENTS

We are indebted to Dr. A.H. De Boer (Vrije Universiteit, Amsterdam) for providing laboratory facilities for the repetition of some experiments on selectivity and for discussions and valuable suggestions, to Dr. U. Hofmann, Göttingen, for advice and support concerning anatomical aspects of the work, to Ms. B. Köhler, Göttingen, for making unpublished data available and for help during the preparation of the manuscript, and to Ms. U. Homann, Göttingen, for helpful comments during the experimental work and on the manuscript. We also thank two anonymous reviewers for their constructive comments and suggestions.

Received December 8, 1993; accepted March 24, 1994.
Copyright Clearance Center: 0032-0889/94/105/0799/15.

LITERATURE CITED

Anderson WP (1976) Transport through roots. *In* U Lüttge, MG Pitman, eds, Encyclopedia of Plant Physiology, New Series, Vol 2, Part B. Springer, Berlin, pp 129–156

Bentrup FW (1990) Potassium ion channels in the plasmalemma. Physiol Plant **79:** 705–711

Cerana R, Colombo R (1992) K^+ and Cl^- conductance of *Arabidopsis thaliana* plasma membrane at depolarized voltages. Bot Acta **105:** 273–277

Clarkson DT (1989) Movements of ions across roots. *In* DY Baker, JL Hall, eds, Solute Transport in Plant Cells and Tissues. Longman Scientific & Technical, Harlow, UK, pp 251–303

Clarkson DT, Hanson JB (1986) Proton fluxes and the activity of a stelar proton pump in onion roots. J Exp Bot **37:** 1136–1150

Cowan DSC, Clarkson DT, Hall JL (1993) A comparison between the ATPase and proton pumping activities of plasma membranes isolated from the stele and cortex of *Zea mays* roots. J Exp Bot **44:** 983–989

Crafts AS, Broyer TC (1938) Migration of salts and water into xylem roots of higher plants. Am J Bot **25:** 529–535

De Boer AH (1985) Xylem/symplast ion exchange: mechanism and function in salt-tolerance and growth. PhD thesis. University of Groningen, The Netherlands

De Boer AH (1989) Xylem transport. Methods Enzymol **174:** 277–287

De Boer AH, Prins HBA (1985) Xylem perfusion of tap root segments of *Plantago maritima*: the physiological significance of electrogenic xylem pumps. Plant Cell Environ **8:** 587–594

Dunlop J (1982) Membrane potentials in the xylem in roots of intact plants. J Exp Bot **22:** 910–918

Dunlop J, Bowling DJF (1971a) The movements of ions to the xylem exudate of maize roots. I. Profiles of membrane potential and vacuolar potassium activity across the root. J Exp Bot **22:** 434–444

Dunlop J, Bowling DJF (1971b) The movement of ions to the xylem exudate of maize roots. III. The location of the electrical and electrochemical potential differences between the exudate and the medium. J Exp Bot **22:** 453–464

Eisenman G, Horn R (1983) Ionic selectivity revisited: the role of

kinetic and equilibrium processes in ion permeation through channels. J Membr Biol **76:** 197–225

Fairley-Grenot KA, Assmann SM (1992) Whole-cell K^+ current across the plasma membrane of guard cells from a grass: *Zea mays*. Planta **186:** 282–293

Führ KJ, Warchol W, Gratzl M (1993) Calculation and control of free divalent cations in solutions used for membrane fusion studies. Methods Enzymol **221:** 149–157

Hamill O, Marty A, Neher E, Sakmann B, Sigworth F (1981) Improved patch-clamp techniques for high-resolution current recording from cells and cell-free membrane patches. Pflügers Arch Eur J Physiol **391:** 85–100

Hanson JB (1978) Application of the chemiosmotic hypothesis to ion transport across the root. Plant Physiol **62:** 402–405

Hedrich R, Busch H, Raschke K (1990) Ca^{2+} and nucleotide dependent regulation of voltage dependent anion channels in the plasma membrane of guard cells. EMBO J **9:** 3889–3892

Hedrich R, Schroeder JI (1989) The physiology of ion channels and electrogenic pumps in higher plants. Annu Rev Plant Physiol **40:** 539–569

Heimsch CH (1951) Development of vascular tissues in barley roots. Am J Bot **38:** 523–537

Hewitt EJ, Smith TA (1975) Plant Mineral Nutrition. English Universities Press, London

Hille B (1992) Ionic Channels of Excitable Membranes. Sinauer Associates, Sunderland, MA

Hylmø B (1953) Transport and ion absorption. Physiol Plant **6:** 333–405

Keller BU, Hedrich R, Raschke K (1989) Voltage-dependent anion channels in the plasma membrane of guard cells. Nature **341:** 450–453

Ketchum KA, Shrier A, Poole RJ (1989) Characterization of potassium-dependent currents in protoplasts of corn suspension cells. Plant Physiol **89:** 1184–1192

Kourie J, Goldsmith MHM (1992) K^+ channels are responsible for an inward rectifying current in the plasma membrane of mesophyll protoplasts from *Avena sativa*. Plant Physiol **98:** 1087–1097

Kramer D (1983) The possible role of transfer cells in the adaptation of plants to salinity. Physiol Plant **58:** 549–555

Läuchli A, Kramer D, Pitman MG, Lüttge U (1974) Ultrastructure of barley roots in relation to ion transport to the xylem. Planta **110:** 85–99

Läuchli A, Spurr AR, Epstein E (1971) Lateral transport of ions into the xylem of corn roots. II. Evaluation of a stelar pump. Plant Physiol **48:** 118–124

Linder B, Raschke K (1992) A slow anion channel in guard cells, activating at large hyperpolarization, may be principal for stomatal closing. FEBS Lett **313:** 27–30

Maathuis FJM, Prins HBA (1990) Patch clamp studies on root cell vacuoles of a salt-tolerant and a salt-sensitive *Plantago* species. Plant Physiol **92:** 23–28

Marrè E (1979) Fusicoccin: a tool in plant physiology. Annu Rev Plant Physiol **30:** 273–288

Moran N, Ehrenstein G, Iwasa K, Mischke C, Bare C, Satter R (1988) Potassium channels in motor cells of *Samanea saman*. Plant Physiol **88:** 643–648

Neher E (1992) Correction for liquid junction potentials in patch clamp experiments. Methods Enzymol **207:** 123–130

Parets-Soler A, Pardo JM, Serano R (1990) Immunolocalization of plasma membrane H^+-ATPase. Plant Physiol **93:** 1654–1658

Pitman MG (1971) Uptake and transport of ions in barley seedlings. I. Estimation of chloride fluxes in cells of excised roots. Aust J Biol Sci **25:** 243–257

Pitman MG (1977) Ion transport into the xylem. Annu Rev Plant Physiol **28:** 71–88

Pitman MG (1982) Transport across plant roots. Q Rev Biophys **15:** 481–554

Robinson RA, Stokes RM (1968) Electrolyte Solutions. Butterworths, London

Schachtman DP, Tyerman SD, Terry BR (1991) The K^+/Na^+ selectivity of a cation channel in the plasma membrane of root cells does not differ in salt-tolerant and salt-sensitive wheat species. Plant Physiol **97:** 598–605

Schroeder JI (1988) K^+-transport properties of K^+-channels in the plasma membrane of *Vicia faba* guard cells. J Gen Physiol **92:** 667–683

Schroeder JI, Raschke K, Neher E (1987) Voltage dependence of K^+ channel currents in guard cell protoplasts. Proc Natl Acad Sci USA **84:** 4108–4112

Spalding EP, Slayman CL, Goldsmith MHM, Gradmann D, Bertl A (1992) Ion channels in *Arabidopsis* plasma membrane. Transport characteristics and involvement in light-induced voltage changes. Plant Physiol **99:** 96–102

Stoeckel H, Takeda K (1989) Calcium-activated voltage-dependent, non-selective anion currents in endosperm plasma membrane from higher plants. Proc R Soc Lond B **237:** 213–231

Stoeckel H, Takeda K (1993) Plasmalemmal, voltage-dependent ionic currents from excitable pulvinar motor cells of *Mimosa pudica*. J Membr Biol **131:** 179–192

Terry BR, Tyerman SD, Findlay GP (1991) Ion channels in the plasma membrane of *Amaranthus* protoplasts—one cation and one anion channel dominate the conductance. J Membr Biol **21:** 223–236

Tester M (1990) Tansley Review No. 21. Plant ion channels: whole-cell and single channel studies. New Phytol **114:** 305–340

Thiel G, MacRobbie EAC, Blatt MR (1992) Membrane transport in stomatal guard cells: the importance of voltage control. J Membr Biol **126:** 1–18

Tyerman SD, Findlay GP (1989) Current-voltage curves of single Cl^- channels which coexist with two types of K^+ channels in the tonoplast of *Chara corallina*. J Exp Bot **40:** 105–117

Van Duijn B, Ypey DL, Libbenga KR (1993) Whole-cell K^+ currents across the plasma membrane of tobacco protoplasts from cell suspension cultures. Plant Physiol **101:** 81–88

Vogelzang SA, Prins HBA (1992) Plasmalemma patch clamp experiments in plant root cells: procedure for fast isolation of protoplasts with minimal exposure to cell wall degrading enzymes. Protoplasma **171:** 104–109

Walker DC, Graham RD (1987) A micro-electrode fast data capture technique: its use to examine plant cell electrophysiology in the wheat root. J Exp Bot **38:** 355–366

Warmbrodt RD (1985) Studies on the root of *Hordeum vulgare* L. Ultrastructure of the seminal root with special reference to the phloem. Am J Bot **72:** 414–432